Erythroblasts highly express the ABC transporter Bcrp1/ABCG2 but do not show the side population (SP) phenotype

journal or publication title	Immunology Letters
volume	114
number	1
page range	52-58
year	2007-11-30
URL	http://hdl.handle.net/2298/9890

doi: 10.1016/j.imlet.2007.08.008

Erythroblasts highly express the ABC transporter Bcrp1/ABCG2 but do not show the side population (SP) phenotype.

Kazumi Yamamoto, Shinya Suzu, Yuka Yoshidomi, Masateru Hiyoshi, Hideki Harada, and Seiji Okada

Division of Hematopoiesis, Center for AIDS Research, Kumamoto University, 2-2-1, Honjo Kumamoto 860-0811, Japan,

Address correspondence to: Seiji Okada M.D., Ph.D., Division of Hematopoiesis, Center for AIDS Research, Kumamoto University, 2-2-1 Honjo, Kumamoto 860-0811, Japan.

Tel: +81-96-373-6522. **FAX:** +81-96-373-6523.

E-mail: okadas@gpo.kumamoto-u.ac.jp

Abstract

Stem cells in various somatic tissues including hematopoietic stem cells can be identified by the “side population (SP)” phenotype based on the efflux of Hoechst33342. Knockout and enforced expression experiments show that the expression of the Bcrp1/ABCG2 gene is an important determinant of the SP phenotype. In this study, we showed that erythroblasts also express a large amount of Bcrp1/ABCG2. The level of expression was increased with maturation, but did not relate to the cell-cycle status. Despite the high expression level of Bcrp1/ABCG2, erythroblasts did not show the “side population” phenotype. Furthermore, a Bcrp1/ABCG2 inhibitor, verapamil, had little effect on the Hoechst33342-staining pattern of erythroblasts. However Protoporphyrin IX fluorescence was significantly higher in the presence of verapamil, suggesting that the ABCG2 functions as a transmembrane transporter in erythroblasts. These results indicate that dissociation between Bcrp1/ABCG2 expression and dye efflux function exists in erythroblasts and in stem cells, and that the function of ABCG2 in erythroblasts differs from that in stem cells.

Key Words: ABCG2; Erythroblast; Hoechst33342; side population;

1. Introduction

Hematopoeitic stem cells can be identified by the "side population (SP)" phenotype, which is based on the efflux of the fluorescent dye Hoechst33342 and can be detected by flow cytometry [1,2]. SP cells have now been identified in many other tissue stem cells of various species as well as cancer stem cells [3,4]. Recently, it has become clear that an ABC transporter, ABCG2 (ATP-binding cassette, subfamily G, member 2), also known as breast cancer resistant protein (Bcrp-1) (Bcrp1/ABCG2), is mainly responsible for the SP phenotype [5-7]. However, ABCG2 is also detected in epithelial tissues such as the placenta, intestine, kidney and hepatic canalicular membrane [4,8]. As for the hematopoietic lineage, previous studies on mouse and human hematopoietic cells demonstrated that ABCG2 is highly expressed in primitive hematopoietic stem cells and is down-regulated in most committed progenitors, and sharply up-regulated during erythroid differentiation [5-7,9,10]. Although the exact physiologic roles of ABCG2 in these cells are not yet well known, it seems likely that an important function of ABCG2 is to protect against the cytotoxic actions of hypoxia or xenotoxins [4, 6, 7, 21].

Here, we report that murine erythroblasts express a large amount of ABCG2; however, they do not show the "SP" phenotype by flowcytometry. Our data demonstrate a clear discrepancy between the expression of ABCG2 and "SP" phenotype and that the function of ABCG2 in erythroblasts differs from that in stem cells.

2. Materials and Methods

2.1.Mice

C57/BL6 mice were purchased from Japan Clea. (Tokyo, Japan) and used in experiments between 8-12 weeks of age. All of the animal experiments were performed according to the guideline in the Institutional Animal Committee of Kumamoto University.

2.2. Monoclonal antibodies (mAbs).

FITC, PE, or APC-conjugated mAbs against Mac-1 (M1-70), TER119 (Ly-76), CD71 (C2), B220 (RA3-6B2), Gr-1 (RB6-8C5), CD34 (RAM34), CD4 (GK1.5) and CD8 (53-6.72) were purchased from BD Pharmingen (San Diego, CA) or eBioscience (San Diego, CA). APC-conjugated anti-Sca-1 (Ly6A/E) and PE-conjugated anti-c-kit (CD117) were purchased from BD Pharmingen and used to purify the primitive hematopoietic stem cell fraction [11].

2.3. Hoechst33342 staining.

Bone marrow (BM) cells were flushed from their femurs with phosphate-buffered saline (PBS) supplemented with 3% fetal calf serum (FCS). The suspension was washed and passed through a 70-micron nylon filter to produce a single-cell suspension. Mature red blood cells were lysed with ACK lysing buffer (0.155M ammonium chloride, 0.1M disodium EDTA, and 0.01M potassium bicarbonate). The BM cells were resuspended at $1x10^6$ cells/ml in 3% FCS/RPMI1640 medium with 5 μg/ml Hoechst33342 (Molecular Probe, Eugene, OR) for 60 min at 37 °C. For the inhibitor experiments, 50μM verapamil (Sigma) was added to cells, and cells were incubated for 15 min at 37 °C, then Hoechst33342 was added [1,2]. The Hoechst-stained cells were resuspended in ice-cold staining medium (PBS with 3% FCS and 0.1% sodium azide) and stained for

30 min on ice with mAbs. Cells were washed and resuspended in staining medium supplemented with 1μg/ml propidium iodide (PI) for flow cytometric analysis and cell sorting.

2.4. Flow cytometric analysis and cell sorting.

Analysis and cell sorting were performed on a triple-laser JSAN flow cytometer (Bay Bioscience, Kobe, Japan) equipped with a 375 nm UV diode laser, 488 nm blue diode laser, and 633 nm red diode laser. The Hoechst33342 dye was excited with 375 nm ultraviolet light and the resultant fluorescence was measured at two wavelengths using 422/44 nm BP and 590/35 nm BP filters for the detection of Hoechst blue and red, respectively. A 530 nm long pass dichroic mirror (DCLP) was used to separate the emission wavelengths. Analysis was also performed on a LSR II flow cytometer (Becton Dickinson, Mountain View, CA) equipped with a 350nm UV diode laser, 408nm violet diode laser, 488nm blue diode laser, and 633nm red diode laser. Multiparameter data were analyzed using the FlowJo program (Tree Star, Ashland, OR).

2.5. RT-PCR analysis. Total RNA was extracted from sorted BM cells using a Trizol Reagent (Gibco BRL, Grand Island, NY). RNAs were reverse-transcribed using Superscript II (Life Technologies, Grand island, NY) and oligo(dT) (Pharmacia, Piscataway, NJ) in a final volume of 20 μl. A Semiquantitative RT-PCR of the ABCG2 transcript in sorted cell populations was performed by amplification of the GAPDH-normalized RT reactions. After an initial 7 min of incubation at 95°C, 30 cycles of PCR were carried out under the following conditions: denaturation at 95°C for 60 sec., annealing at 60°C for 40 sec, and polymerization at 72°C for 60 sec. Primers for

the cDNA amplification were as follows: ABCG2 primers, 5'-CCATAGCCACAGGCCAAAGT-3' and 5'-GGGCCACATGATTCTTCCAC-3'; G3PDH primers, 5'-TGAAGGTCGGTGTGAACGGATTTGGC-3' and 5'-CATGTAGGCCATGAGGTCCACCAC-3'. The PCR products were separated on a 1.2 % agarose gel and stained with ethidium bromide.

2.6. Real time PCR.

Real time PCR was performed on a Thermal Cycler Dice Real Time System (Takara Bio., Japan) using a SYBERExScript RT-PCR kit (Takara Bio.) according to manufacturer's instruction. The primers used for real time PCR were designed by Takara Bio: ABCG2, MA030903; GAPDH, MA023937.

2.7. Western blot analysis.

Total proteins from sorted cells were extracted with RIPA buffer. Lysates were clarified by centrifugation. Samples were electrophoresed through 7.5% SDA-PAGE gels and transferred to a nylon membrane (Hybond-P, GE Healthcare Bio-Science, NJ). After blocking with Block Ace (Dainippon Sumitomo Pharma, Japan), the membrane was reacted with a 1/100 dilution of anti-ABCG2 antibody (BXP-53) (Monosan, The Netherlands) for 1 hr at room temperature. Detection was performed using the Enhanced Chemiluminescence Western Blotting Detection System (ECL, GE Healthcare Bio-Science) with HPR-conjugated Goat anti-rat immunoglobulins (Dako).

2.8. Cellular Protoporphyrin IX (PPIX) measurements

Cellular PPIX concentration was measured as described previously [10]. For PPIX efflux assays, cells were incubated with 10 mM PPIX (Sigma) in 10%FCS/DMEM for

30 min at 37 °C, washed once with medium, and incubated at 37 °C for 1 hour. Verapamil (50μM), if used, was present during the entire procedure. Cells were spun down, resuspended into staining medium, and analyzed in a flow cytometry (LSR II) for PPIX fluorescence using a 695/40-nm filter after excitation by a 408 nm Violet light. For endogenous PPIX assays, BM cells were treated with 1mM δ-aminolevulinic acid (ALA) (Sigma) for 21 hours, washed once with PBS, stained with TER119-APC and CD71-FITC, and directly analyzed in a LSR II flow cytometry for PPIX fluorescence.

3. Results and Discussion

3.1 Erythroblasts express high levels of ABCG2 mRNA and Protein.

Although ABCG2 is responsible for the SP phenotype, it is known to be expressed in cells other than stem cells [4, 5]. As for the hematopoietic lineage, hematopoietic stem cells, erythroblasts, and NK cells express ABCG2 [5, 10, 12]. To determine the level of expression of ABCG2 in bone marrow cells, a subpopulation of bone marrow and spleen cells was isolated by flow cytometric sorting. RT-PCR analysis showed that ABCG2 mRNA was present in the erythroid lineage ($TER119^{+}$ cells) but little expressed in the myeloid, B lymphoid and T lymphoid lineages (Fig.1A). Western blot analysis showed that ABCG2 protein was present only in erythroblasts (Fig.1B).

Erythroblasts can be divided into four subsets (R1: $TER119^{low}CD71^{high}$, R2: $TER119^{high}CD71^{high}$, R3: $TER119^{high}CD71^{med}$, R4: $TER119^{high}CD71^{low\text{-}negative}$) based on simultaneous immunostaining with anti-TER119 and anti-CD71 mAbs (Fig.1C) [13,14]. Erythroblasts sequentially differentiate from proerythroblasts (R1) into basophilic erythroblasts (R2), polychromatophilic erythroblasts (R3), and orthochromatophilic

erythroblasts and reticulocytes (R4) [14]. Semiquantative RT-PCR revealed that the level of expression of ABCG2 mRNA was higher at all stages in erythroblasts than in the hematopoietic stem cell fraction (KSL cells) (Fig. 1D). This explains why less than 10% of KSL cells are $CD34^-$ primitive hematopoietic stem cells highly expressing ABCG2 and with the differentiation into $CD34^+$KSL cells, they lose ABCG2 expression rapidly [5]. To further assess the expression of ABCG2 mRNA, real time RT-PCR was performed. As shown in Fig.1E, the ABCG2 mRNA level increased with the erythroid maturation. Our data obtained with fresh erythroblasts were consistent with the results of Zhou et al [5,10], who showed that ABCG mRNA expression is up-regulated with erythroid maturation using erythroid cell lines, MEL and K562, and cultured erythroblasts. It is interesting note that the expression of ABCG2 mRNA was high in erythroblasts as in $CD34^-$KSL cells. These data are in consistent with the ABCG2 knock in mouse study, in which GFP expression was observed only in TER119 positive cells and hematopoietic stem cells [15]

3.2. Erythroblasts do not show the SP phenotype in spite of high expression of ABCG2..

To further analyze the relationship between ABCG2 expression and the SP phenotype, we stained the bone marrow cells with Hoechst33342, Sca-1-FITC, c-kit-APC, and TER119-PE, simultaneously, analyzed them using flow cytometry, and drew up plots of Hoechst33342 red/blue fluorescence. Whole BM cells had the SP phenotype as previously described [1], and most cells with the SP phenotype were positive for Sca-1 and c-kit (Fig. 2A), but negative for Mac-1, B220, and TER119 (data not shown). In

contrast, TER119$^+$ cells did not have the SP phenotype (Fig.2B). These results clearly demonstrate the dissociation between ABCG2 expression and the dye-efflux function of ABCG2. As Hoechst33342 can be excited with a UV laser and is a cell membrane-permeant DNA-selective binding dye, it was originally used in cell-cycle studies [16]. TER119$^+$ cells were divided into three fractions based on the pattern of staining by Hoechst blue (Fig.2B), i.e. subdiploid (G1), G0/G1 phase (G2) and S/G2/M phase (G3). We compared the expression levels of ABCG2 by semiquantitative RT-PCR. As shown in Fig.2C, ABCG2 mRNA expression was not linked to the cell cycle state of erythroblasts.

ABCG2 has been identified as responsible for the SP phenotype [5]. In fact, overexpression of ABCG2 increased the SP phenotype [5], and mice deficient in ABCG2 lacked the side population in bone marrow [6]. Since then, the SP phenotype has been used as a stem cell marker and to isolate the stem cell fraction. However, Morita et al. recently demonstrated the existence of a non-SP ABCG2-expressing hematopoietic stem cell fraction [17]. Their data imply a dissociation between ABCG2 expression and the dye-efflux function of Bcrp1/ABCG2.

3.3. Effects of an ABCG inhibitor, verapamil, on Hoechst33342 staining pattern and protoporphyrin IX efflux of erythroid lineage.

The SP phenotype is caused by the active efflux of Hoechst33342 via ABCG2 [5], and this mechanism can be inhibited by ABC transporter inhibitors [1, 2]. To determine whether ABCG2 activity was involved in the phenotype of the erythroid lineage, the effect of verapamil, an ABCG2 inhibitor, was assessed. The SP fraction was markedly

reduced in the presence of this ABC transporter inhibitor (50 μg/ml), as expected (Fig.3). On the other hand, verapamil did not affect the Hoechst33342 staining patterns of both ABCG2 negative myeloid (Mac-1^{+}) and ABCG2 positive erythroid (TER119^{+}) cells, suggesting that although ABCG2 is highly expressed in erythroid cell, it dose not work for effective pump in erythroblasts. In order to determine if endogenously expressed ABCG2 in erythroid cells work effectively or not, we analyzed the effect of verapamil for efflux of exogenous protoporphilin IX (PPIX), as PPIX is the direct and natural substrate for ABCG2 [10]. Murine BM cells were incubated with PPIX with or without verapamil, and PPIX fluorescence was determined by flow cytometry. The PPIX fluorescence was significantly higher in the presence of verapamil (Figure 4), showing that ABCG2 functions as effective transporter in primary erythroblasts. Although the PPIX fluorescence level differed, the PPIX fluorescence was significantly higher in the presence of verapamil in all of the erythroid subfractions. This result was confirmed with another experiment (Figure 4) in which BM cells were treated with δ-ALA, which produce endogenous PPIX in erythroid cells. These results indicate that although ABCG2 is functionally expressed in erythroid cells, the function of ABCG2 in erythroblasts differs from that in stem cells. Such speculation is supported by reports that hematopoietic stem cells are relatively resistant to anticancer reagents such as 5-FU compared to the erythroid lineage [18,19]. In addition, Zong et al. demonstrated that the expression of ABCG2 during hematopoiesis is transcriptionally regulated by the alternative use of multiple leader exons and promoters in a developmental stage-specific manner [20]. In their observation, the expression patterns of ABCG2 mRNA isoforms

were different between murine hematopoietic stem cells and erythroid cells.

ABCG2-deficient mice developed by Jonker et al. appeared normal, and hematocrit and hemoglobin levels were compatible between the wild-type and ABCG2-deficient mice [21], suggesting normal activity of heme synthesis-related enzymes under steady state conditions. Recently, Krishnamurthy et al. showed that ABCG2 specifically bound heme, and enhanced hypoxic cell survival [22]. They also demonstrated that ABCG2 expression was up-regulated by hypoxia, which involved the hypoxia-inducible transcription factor complex HIF-1. These mechanisms are largely responsible for the survival of hematopoietic stem cells in the hypoxic osteoblastic niche [23, 24]. But it is unclear whether this mechanism works in erythroblasts or not. Also, it is unknown why ABCG2 does not function in the efflux of Hoechst33342 dye in erythroblasts. One possible explanation is that since erythroblasts contain a large amount of heme, most of the ABCG2 binds with heme [22] and heme bound ABCG2 may not function as a transmembrane transporter. This is supported by the fact that the expression of ABCG2 is up-regulated with erythroid differentiation, since the synthesis of heme also increases with erythroid differentiation [25]. Another explanation is that although ABCG2 expression is essential for Hoechst dye efflux, additional gene is needed to exhibit the "side population" which lack in erythroblasts. This is supported by the fact that erythroid cells and hematopoietic stem cells use different promoters to control the initiation of ABCG2 transcription [20], and therefore it is controlled by different mechanisms.

In summary, we showed that freshly isolated murine erythroblasts highly expressed

functional ABCG2 but did not exhibit the “side population” phenotype, suggesting that ABCG2 is necessary but not sufficient for the exhibition of “side population”. Further investigation of the functional role of ABCG2 signaling and its molecular mechanisms, especially differences between stem cells and erythroblasts, will provide a clue as to how stem cells are maintained and regulated by membrane transporters.

Acknowledgments

We are grateful to Ms. Y Endo for secretarial assistance, and Ms. I. Suzu for skillful technical assistance. This work was supported in part by Health and Labour Sciences Research Grants from the Ministry of Health, Labour and Welfare of Japan and by grants from the Ministry of Education, Science, Sports, and Culture of Japan.

References

[1] Goodell MA, Brose K, Paradis G, Conner AS, Mulligan RC. Isolation and functional properties of murine hematopoietic stem cells that are replicating in vivo. J Exp Med 1996;183:1797-1806.

[2] Goodell MA, Rosenzweig M, Kim H, Marks DF, Demaria M, Paradis G, Grupp SA, Sieff CA, Malligan RC, Johnson RP. Dye efflux studies suggest that hematopoietic stem cells expressing low or undetectable levels of CD34 antigen exist in multiple species. Nat Med 1997;3:1337-1345.

[3] Challen GA, Little MH. A side order of stem cells: the SP phenotype. stem cells

2006;24:3-12.

[4] Doyle LA, Ross DD. Multidrug resistance mediated by the breast cancer resistant protein BCRP (ABCG2). Oncogene 2003;22:7340-7358.

[5] Zhou S, Schuetz JD, Bunting KD, Colapietro AM, Sampath J, Morris JJ, Lagutina I, Grosveld GC, Osawa M, Nakauchi H, Sorrentino BP. The ABC transporter Bcrp1/ABCG2 is expressed in a wide variety of stem cells and is a molecular determinant of the side-population phenotype. Nat Med 2001;7:1028-1034.

[6] Zhou S, Morris JJ, Barnes Y, Lan L, Schuetz JD, Sorrentino BP. Bcrp1 gene expression is required for normal numbers of side population stem cells in mice, and confers relative protection to mitoxantrone in hematopoietic cells in vivo. Proc Natl Acad Sci USA 2002;99:12339-12344.

[7] Scharenberg CW, Harkey MA, Torok-Storb B. The ABCG2 transporter is an efficient Hoechst 33342 efflux pump and is preferentially expressed by immature human hematopoietic progenitors. Blood 2002;99:507-512.

[8] Staud F, Pavek P. Breast cancer resistance protein (BCRP/ABCG2). Int J Biochem Cell Biol 2005;37:720-725.

[9] Tadjali M, Zhou S, Rehg J, Sorrentino BP. Prospective isolation of murine hematopoietic stem cells by expression of an Abcg2/GFP allele. Stem Cells 2006;24:1556-1563.

[10] Zhou S, Zong Y, Ney PA, Nair G, Stewart CF, Sorrentino BP. Increased expression of the Abcg2 transporter during erythroid maturation plays a role in decreasing cellular protoporphyrin IX levels. Blood 2005;105:2571-2576.

[11] Okada S, Nakauchi H, Nagayoshi K, Nishikawa S, Miura Y, Suda T. In vivo and in vitro stem cell function of c-kit- and Sca-1-positive murine hematopoietic stem cells. Blood 1992;80:3044-3050.

[12] Pearce DJ, Ridler CM, Simpson C, Bonnet D. Multiparameter analysis of murine bone marrow side population cells. Blood 2004;103:2541-2546.

[13] Socolovsky M, Nam H, Fleming MD, Haase VH, Brugnara C, Lodish HF. Ineffective erythropoiesis in Stat5a$^{-/-}$5b$^{-/-}$ mice due to decreased survival of early erythroblasts. Blood 2001;98:3261-3273.

[14] Asari S, Sakamoto A, Okada S, Ohkubo Y, Arima M, Hatano M, Kuroda Y, Tokuhisa T. Abnormal erythroid differentiation in neonatal bcl-6-deficient mice. Exp Hematol 2005;33:26-34.

[15] Tadjall M, Zhou S, Rehg J, Sorrentino BP. Prospective isolation of murine hematopoietic stem cells by expression of an Abcg2/GFP allele. Stem Cells 2006;24:1556-1563.

[16]Shapiro HM. Flow cytometry of DNA content and other indicators of proliferative activity. Arch Pathol Lab Med 1989;113:591-597.

[17] Morita Y, Ema H, Yamazaki S, Nakauchi H. Non-side-population hematopoietic stem cells in mouse bone marrow. Blood 2006;108:2850-2856.

[18] Zant GV. Studies of hematopoietic stem cells spared by 5-fluorouracil. J Exp Med 1984;159:679-690.

[19] Weiterova L, Hofer M, Pospisil M, Znojil V, Vacha J, Vacek A, Pipalova I. Influence of the joint treatment with granulocyte colony-stimulating factor and drugs

elevating extracellular adenocine on erythropoietic recovery following 5-fluorouracil-induced haematotoxicity in mice. Eur J Haematol 2000;65:310-316.

[20] Zong Y, Zhou S, Fatima S, Sorrentino BP. Expression of mouse Abcg2 mRNA during hematopoiesis is regulated by alternative use of multiple leader exons and promoters. J Biol Chem 2006;281:29625-29632.

[21] Jonker JW, Buitelaar M, Wagenaar E, van der Valk MA, Scheffer GL, Scheper RJ, Plösch T, Kuipers F, Oude Elferink RPJ, Rosing H, Beijnen JH, Schinkel AH. The breast cancer resistance protein protects against a major chlorophyll-derived dietary phototoxin and protoporphyria. Proc Natl Acad Sci USA 2002;99:15649-15654.

[22] Krishnamurthy P, Ross DD, Nakanishi T, Bailey-Dell K, Zhou S, Mercer KE, Sarkadi B, Sorrentino BP, Schuetz JD. The stem cell marker Bcrp/ABCG2 enhances hypoxic cell survival through interactions with heme. J Biol Chem 2004;279:24218-24225.

[23] Yin T, Li L. The stem cell niches in bone. J Clin Invest 2006;116:1195-1201.

[24] Suda T, Arai F, Hirao A. Hematopoietic stem cells and their niche. Trends Immunol 2005;26:426-433.

[25] Schranzhofer M, Schifrer M, Cabrera JA, Kopp S, Chiba P, Beug H, Mullner EW. Remodeling the regulation of iron metabolism during erythroid differentiation to ensure efficient heme biosynthesis. Blood 2006;107:4159-4167.

[26] Nakajima O, Takahashi S, Harigae H, Furuyama K, Hayashi N, Sassa S, Yamamoto M. Heme deficiency in erythroid lineage causes differentiation arrest and cytoplasmic iron overload. EMBO J 1999;18:6282-6289.

Figure Legends

Figure 1. Expression of ABCG2 in the erythroblast subsets.

(A) ABCG2 mRNA expression was analyzed in erythroid cells ($TER119^{+}$), myeloid cells ($Mac\text{-}1^{+}$), B lymphoid cells ($B220^{+}$) and T lymphoid cells ($Thy\text{-}1^{+}$) isolated from BM or spleen. (B) Western blot analysis of the ABCG2 protein in erythroid cells ($TER119^{+}$), myeloid cells ($Mac\text{-}1^{+}$) and B lymphoid cells ($B220^{+}$) isolated from BM. (C) The BM cells were stained with anti-TER119 and anti-CD71 mAbs and analyzed using a JSAN flow cytometer. Erythroblasts sequentially differentiate from R1 ($TER119^{low}CD71^{high}$) into R2 ($TER119^{high}CD71^{high}$) cells, R3 ($TER119^{high}CD71^{med}$) cells, and R4 ($TER119^{high}CD71^{low\text{-}negative}$) cells. (D) ABCG-2 expression was analyzed by semiquantitative RT-PCR in immature to mature erythroblasts (R1 to R4), the hematopoeitic stem cell fraction ($Lin^{-}c\text{-}kit^{+}Sca\text{-}1^{+}$) and myeloid ($Mac\text{-}1^{+}$) cells. cDNAs serially diluted 8 times were used for PCR. Results are representative of three independent experiments. (E) ABCG2 expression was analyzed by real-time PCR in immature to mature erythroblasts (R1 to R4), the hematopoietic stem cell fraction ($Lin^{-}c\text{-}kit^{+}Sca\text{-}1^{+}$) and myeloid ($Mac\text{-}1^{+}$) cells. The copy numbers of ABCG2 mRNA were quantified by comparison with a standard curve. Values were normalized to mouse G3PDH expression, which was used as the endogenous control.

Figure 2. Erythroblasts do not show the SP phenotype but highly express ABCG2 mRNA.

Whole BM cells were stained with Hoechst33342, followed by c-kit-FITC, Sca-1-APC

and TER119-PE, and analyzed on a flow cytometry. (A) A display of whole BM cells on a Hoechst red/blue plot reveals the side population. In contrast, $TER119^+$ cells contained very few SP cells. (B) $TER119^+$ cells are divided into three fractions based on the pattern of staining by Hoechst blue, i.e.: subdiploid (G1), G0/G1 phase (G2), and S/G2/M phase (G3). (C) The expression of ABCG2 was examined by RT-PCR. cDNA was synthesized from total RNA extracted from the three sorted erythroid fractions (G1, G2, and G3), the hematopoietic stem cell fraction ($Lin^-c\text{-}kit^+Sca\text{-}1^+$), and myeloid ($Mac\text{-}1^+$) cells. cDNAs serially diluted 8 times were used for PCR. Results are representative of three independent experiments.

Figure 3. Influence of verapamil (an ABCG2 inhibitor) on the Hoechst red/blue profile of whole BM, myeloid ($Mac\text{-}1^+$), and erythroid ($TER119^+$) cells.

Whole BM cells were stained with Hoechst33342 in the presence or absence of verapamil, followed by Mac-1-FITC and TER119-PE., and analyzed on a flow cytometry. A display of whole BM cells on a Hoechst red/blue plot reveals the side population (SP). The SP fraction (R1) disappeared in the presence of verapamil, but it had no influence on the Hoechst red/blue profile of myeloid ($Mac\text{-}1^+$) and erythroid ($TER119^+$) cells.

Figure 4. Influence of verapamil on the endogenous and exogenous efflux of PPIX from erythroblasts.

BM cells were incubated with (A) δ-ALA or (B) PPIX, with verapamil (solid line) or

without verapamil (shaded area) and analyzed for PPIX fluorescence of erythroblast subfraction. The numbers in the graph show the mean fluorescence intensity (MFI) of PPIX fluorescence without/with verapamil. In all erythroblasts subfraction, PPIX fluorescence was significantly increased by treatment with verapamil.

Figure 1

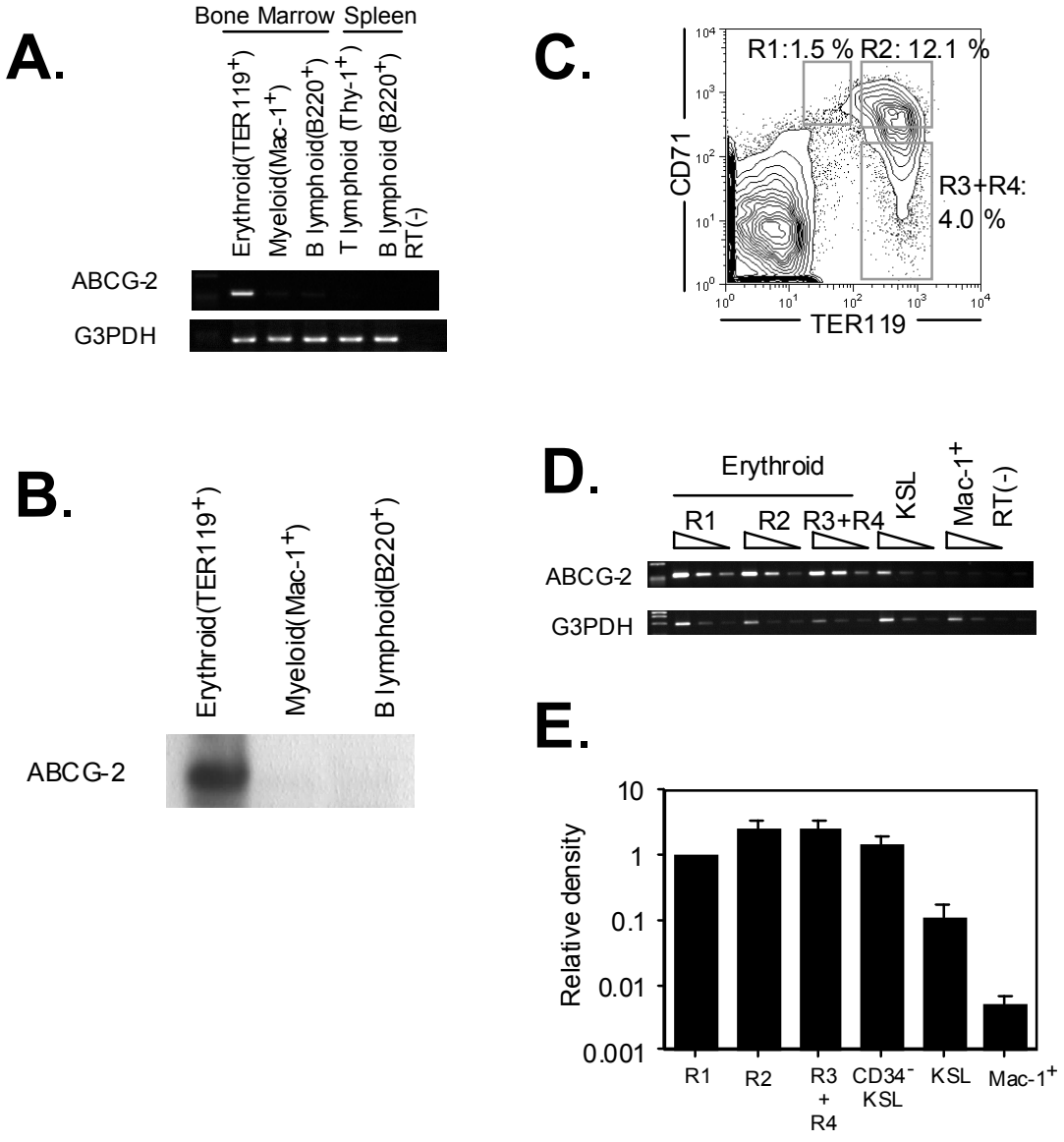
A.
Bone Marrow
Spleen
Erythroid(TER119+)
Myeloid(Mac-1+)
B lymphoid(B220+)
T lymphoid (Thy-1+)
B lymphoid (B220+)
RT(-)
ABCG-2
G3PDH
B.
Erythroid(TER119+)
Myeloid(Mac-1+)
B lymphoid(B220+)
ABCG-2
C.
R1:1.5 %
R2: 12.1 %
R3+R4:
4.0 %
CD71
TER119
D.
Erythroid
R1
R2
R3+R4
KSL
Mac-1+
RT(-)
ABCG-2
G3PDH
E.
Relative density
10
1
0.1
0.01
0.001
R1
R2
R3 + R4
CD34- KSL
KSL
Mac-1+

Figure 2

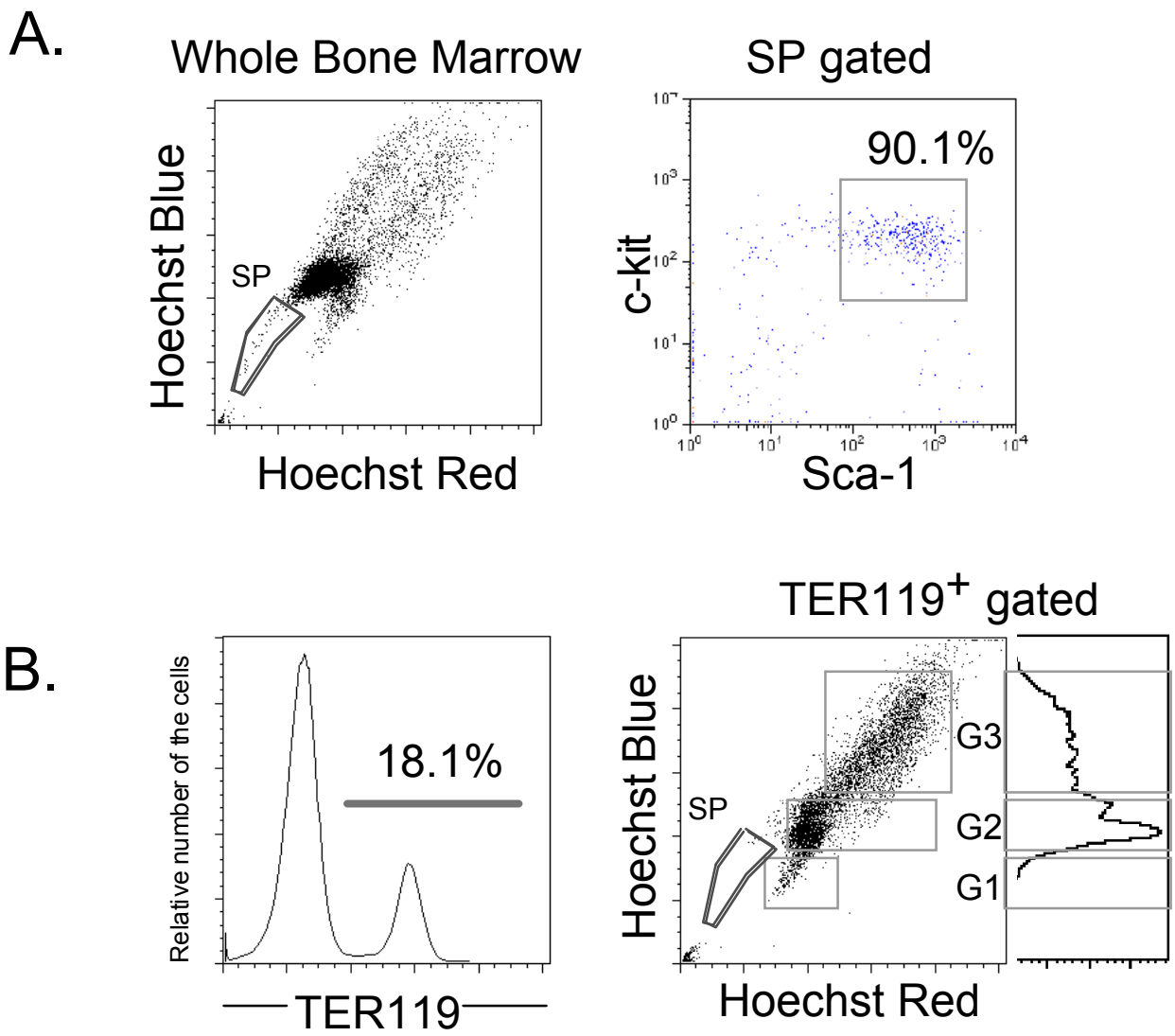
A.
Whole Bone Marrow
SP gated
Hoechst Blue
Hoechst Red
SP
90.1%
c-kit
Sca-1
B.
TER119+ gated
Relative number of the cells
18.1%
TER119
Hoechst Blue
Hoechst Red
SP
G3
G2
G1
C.
TER119+ cells
G1
G2
G3
KSL
Myeloid
RT(-)
ABCG-2
G3PDH

Figure 3

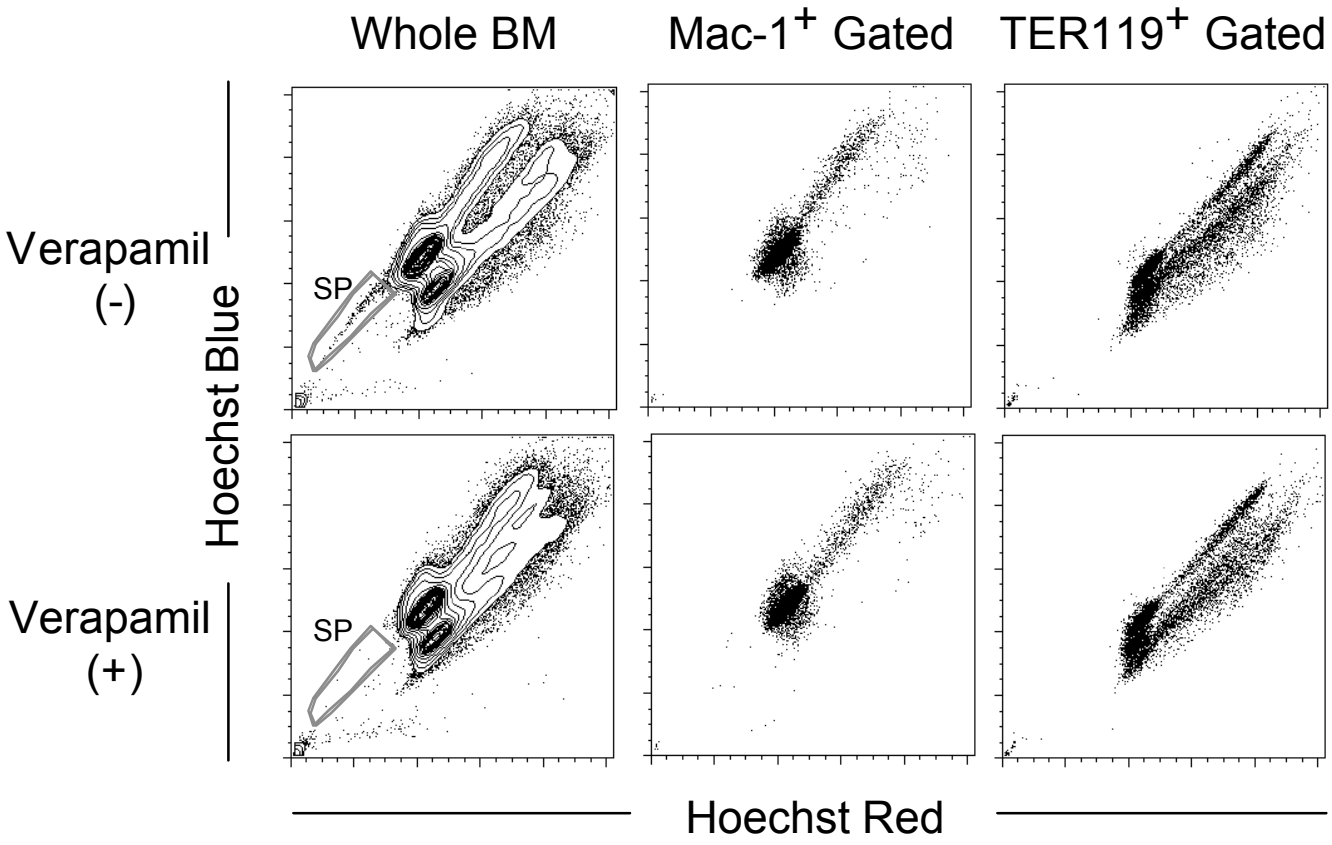
Whole BM
Mac-1+ Gated
TER119+ Gated
Verapamil (-)
Verapamil (+)
SP
SP
Hoechst Blue
Hoechst Red

Figure 4

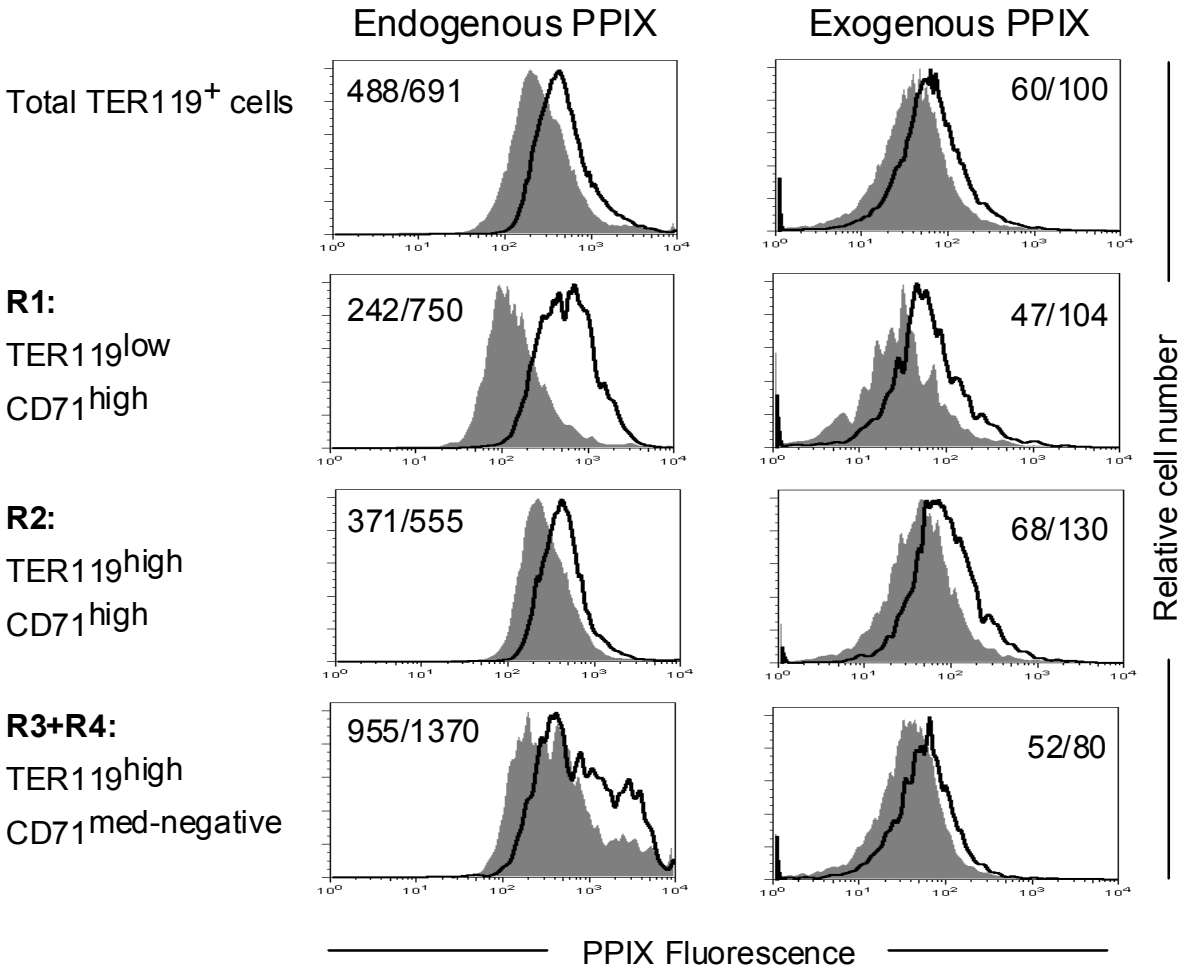
Endogenous PPIX
Exogenous PPIX
Total TER119+ cells
488/691
60/100
R1:
TER119low
CD71high
242/750
47/104
R2:
TER119high
CD71high
371/555
68/130
R3+R4:
TER119high
CD71med-negative
955/1370
52/80
Relative cell number
PPIX Fluorescence